AGU PUBLICATIONS

JGR

Journal of Geophysical Research: Space Physics

RESEARCH ARTICLE

10.1002/2013JA018937

Key Points:
- The total duration and number of Bs events follow sunspot number as $Bz < -5$ nT
- In great Bs events, 53% are related to MC and 10% are related with ejecta
- Bs events with similar duration and value, Earth's responses could be different

Correspondence to:
X.-Y. Zhang,
zhangxy@umich.edu

Citation:
Zhang, X.-Y., and M. B. Moldwin (2014), The source, statistical properties, and geoeffectiveness of long-duration southward interplanetary magnetic field intervals, *J. Geophys. Res. Space Physics*, *119*, 658–669, doi:10.1002/2013JA018937.

Received 12 APR 2013
Accepted 15 AUG 2013
Accepted article online 20 JAN 2014
Published online 6 FEB 2014

The source, statistical properties, and geoeffectiveness of long-duration southward interplanetary magnetic field intervals

X.-Y. Zhang[1] and M. B. Moldwin[1]

[1]Department of Atmospheric, Oceanic, and Space Sciences, University of Michigan, Ann Arbor, Michigan, USA

Abstract Geomagnetic activity is strongly controlled by solar wind and interplanetary magnetic field (IMF) conditions, especially the southward component of IMF (IMF Bs). We analyze the statistical properties of IMF Bs at 1 AU using in situ observations for more than a solar cycle (1995–2010). IMF Bs events are defined as continuous IMF Bs intervals with varying thresholds of Bs magnitude and duration and categorized by different solar wind structures, such as magnetic cloud (MC), interplanetary small-scale magnetic flux rope, interplanetary coronal mass ejection without MC signature (ejecta), stream interacting region, and Shock, as well as events unrelated with well-defined solar wind structures. The statistical properties of IMF Bs events and their geoeffectiveness are investigated in detail based on satellite and ground measurements. We find that the integrated duration and number of Bs events follow the sunspot number when $Bz < -5$ nT. We also find that in extreme Bs events ($t > 6$ h, $Bz < -10$ nT), a majority (53%) are related to MC and 10% are related with ejecta, but nearly a quarter are not associated with any well-defined solar wind structure. We find different geomagnetic responses for Bs events with comparable duration and magnitude depending on what type of solar wind structures they are associated with. We also find that great Bs events ($t > 3$ h, $Bz < -10$ nT) do not always trigger magnetic storms.

1. Introduction

The relationship between interplanetary magnetic field (IMF) *z* component (*Bz*) and geomagnetic activity has been extensively studied since the introduction of the concept of magnetic reconnection as the driver of magnetospheric dynamics [e.g., *Dungey*, 1961] and the first systematic observations of the upstream solar wind conditions. *Fairfield and Cahill* [1966] found that the southward component of IMF is associated with ground magnetic disturbances on Earth while the northward component corresponds to quiet geomagnetic conditions. *Arnoldy* [1971] showed that the solar wind/IMF parameter best correlated with auroral electrojet index (*AE*) is the preceding time integral of IMF southward component (Bs); thus, he suggested that IMF Bs represents a continuing dynamic mechanism for the production of substorms rather than just being a trigger. Later, *Akasofu* [1979] found that the most important parameters in the solar wind controlling the development of the main phase of geomagnetic storms and substorms are a combination of solar wind speed, magnetic field magnitude (Bt), and its polar angle.

Strong IMF Bs is often observed in solar wind structures such as high-speed streams (HSS) from coronal holes (CHs) [*Sheeley et al.*, 1976], coronal mass ejections (CMEs) [*Klein and Burlaga*, 1982; *Lindsay et al.*, 1995], interplanetary small-scale magnetic flux ropes (ISMFRs) [*Moldwin et al.*, 2000; *Feng et al.*, 2010; *Zhang et al.*, 2012], and corotating interaction regions (CIRs) [*Rosenberg and Coleman*, 1980]. Based on the classic theory of the generation and evolution of IMF, large-amplitude southward component intervals should be mostly found in these structures [*Dessler*, 1967]. Thus, the properties and geoeffectiveness of these solar wind structures have been widely studied. *Webb* [1991] and *Yashiro et al.* [2004] have found that the occurrence rate of CMEs peaks strongly during solar maximum, while CIR peaks during the late declining phase of the solar cycle [*Mursula and Zieger*, 1996]. The interaction regions produced by nonrecurrent HSS occur throughout the solar cycle [*Bobrov*, 1983; *Jian et al.*, 2011]. *Jian et al.* [2006b] defined Interplanetary CME (ICME) mainly based on perpendicular pressure and suggested that at 1 AU, a Magnetic Cloud (MC) is observed during spacecraft crossings for only one third of ICMEs. *Gosling* [1993], *Xu et al.* [2009], and *Richardson and Cane* [2012] showed that CIRs were more important for inducing moderate and small storms while MCs triggered intense storms more frequently. *Echer et al.* [2008] found that *Dst* has the highest dependence on the

integrated Bs or Ey (product of Bs and Vx) than other interplanetary components. Besides the well-defined solar wind structures, there are discontinuities (tangential and rotational discontinuities and slow shocks) related with Bs events. *Burlaga* [1968] showed that directional discontinuities in the interplanetary medium are always accompanied with a change of the direction normal to the ecliptic plane, which is IMF *z* component most of the time.

Geomagnetic storms with minimum *Dst* less than −100 nT are found to be almost always caused by strong negative *Bz* with durations longer than 3 h [*Gonzalez et al.*, 1994]. Many studies have also shown that the magnitude of geomagnetic storms increases with either more intense or longer southward IMF [e.g., *Hirshberg and Colburn*, 1969; *Arnoldy*, 1971].

Geomagnetic substorms were initially considered to be a simultaneous phenomenon with storms but weaker in effect, and *Akasofu* [1968] showed that a chain of substorms could induce storm-time ring current. However, *Tsurutani and Gonzalez* [1987] confirmed that ongoing substorm activity does not necessarily lead to storms, and more recent studies demonstrated that substorms can be triggered by internal sources [*Horwitz*, 1985; *Henderson et al.*, 1996] or external driving factors such as certain configurations of IMF [e.g., *Heppner*, 1955; *Lyons*, 1995; *Zhou and Tsurutani*, 2001]. *Burch* [1972], *Samson and Yeung* [1986], and *Lyons* [1996] have found that the northward turning of the IMF can trigger substorm onset.

Since it is highly correlated with solar wind/IMF conditions, the current prediction of geomagnetic activity, especially large-scale storms, is based on the forecast of occurrence of geoeffective solar activity and the ensuing solar wind and IMF conditions. The maximum magnitude of IMF Bs observed in situ at 1 AU was found to be directly related with the propagation velocity of CMEs observed in coronagraph observations [*Lindsay et al.*, 1999]. This velocity is needed for forecasting the arrival time of ICME to the Earth [*Hochedez et al.*, 2005]. Further, though the occurrence frequency and time delay of CH outflows or CIR are easily estimated, the determination of the Sun-Earth magnetic connectivity is unfortunately not straightforward [*Schwadron and McComas*, 2004] and requires the knowledge of the instantaneous Parker spiral geometry and a comprehensive understanding of IMF *Bz* evolution. Despite the progress in space weather modeling, predicting IMF Bs at 1 AU is still poorly done [*Hochedez et al.*, 2005].

In this study, we analyze the 1 min magnetic field data at 1 AU from 1995 to 2010 to obtain the characteristics of IMF Bs events (defined as continuous periods of southward IMF with different criteria of duration and magnitude). We also investigate the properties of IMF Bs events and their geoeffectiveness in different types of solar wind structures, such as MC, ICME without MC signature, ISMFR, stream interacting region (SIR, which includes CIR), and Shock, as well as intervals not associated with well-defined solar wind structures. The knowledge of the statistical properties of IMF Bs at 1 AU is important in examining their source and propagation to improve the prediction capability of the interplanetary magnetic field in the near-Earth region from remote sensing measurements, which will then provide more realistic input of solar wind/IMF conditions to magnetosphere-ionosphere models.

2. Methodology

In order to study the statistical properties and geoeffectiveness of IMF southward component, we examine the 1 min WIND/OMNI magnetic field data at 1 AU from 1995 to 2010 (data source: *http://cdaweb.gsfc.nasa.gov/istp_public/*). We define and select Bs events as follows:

1. Setting the maximum values of IMF *Bz* in GSE coordinates from 0 nT to −10 nT decreasing by 1 nT each step and automatically identifying the intervals with at least three satisfactory points (3 min duration), ignoring single points between two intervals that meet the requirement;
2. Setting the minimum values of the duration from 3 min to 6 h increasing by 10 min each step and selecting the Bs events from step (1). Figure 1 shows a schematic example about how we accept and reject an interval as a Bs event. The intervals from time point 5 to point 12 and from time point 15 to time point 18 are considered as Bs events with thresholds as −5 nT and 3 mins.

Based on the yearly distribution of the number and total duration of the Bs events selected out by different thresholds of *Bz* magnitude and duration, we found that yearly sunspot number shows similar trend as Bs events when the maximum value of *Bz* magnitude is smaller than −3 nT and minimum value of duration is larger than 1 h.

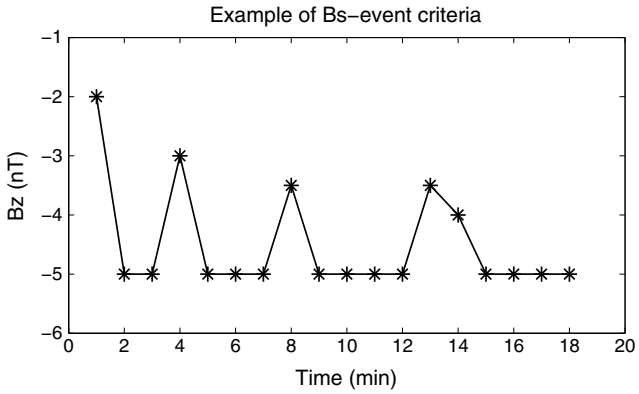

Figure 1. A schematic example about how we accept and reject an interval as a Bs event. The intervals from time point 5 to points 12 and from time point 15 to time point 18 are considered as Bs events with thresholds as −5 nT and 3 mins.

Compared with previous studies of different solar wind structures (SIR, ISMFR, ejecta [*Jian et al.*, 2006a; *Feng et al.*, 2008; *Jian et al.*, 2011; *Richardson and Cane*, 2012], and published lists of Interplanetary Shock Database from Center for Astrophysics and Lepping Magnetic Cloud), we categorize the Bs events from the WIND IMF data (if WIND satellite was crossing the Earth's magnetosphere, we averaged ACE/IMP 8 magnetic field data into 1 min resolution instead of WIND data) into MC, ISMFR, ICME without MC signature (hereafter referred to as ejecta, [*Burlaga et al.*, 2001]), SIR, and Shock if there is an overlap between a Bs event and a solar wind structure. If there is no overlap, we define the Bs event as unrelated with well-defined solar wind structures.

For the MC list, the start and end times were estimated by a magnetic field model [*Lepping et al.*, 1990], assuming that the field within the magnetic cloud is force free using Magnetic Fields Investigation (MFI) data from WIND. For SIR list, the authors calculated the total perpendicular pressure (the sum of the magnetic pressure and plasma thermal pressure perpendicular to the magnetic field) for the WIND and ACE data set and defined the boundary from a combination of signatures described in their paper [*Jian et al.*, 2006a]. The main requirement is that the interval covers where the pressure structure emerges from then decays back to the background. The interplanetary shocks were analyzed using plasma data from Solar Wind Experiment and MFI onboard WIND spacecraft based on the criteria that increases of at least 3%, 20%, and 30% sharply occur in bulk speed, IMF magnitude, and density of downstream compared to the upstream values. The immediate 20 min of data on either side of the shock is used to characterize the upstream and downstream plasma parameters [*Jurac et al.*, 2002]. For the ejecta list, the authors set up the boundaries of the events mainly based on a consensus of the solar wind plasma and magnetic field signatures [*Cane and Richardson*, 2003; *Richardson and Cane*, 2012]. The ISMFRs were preselected out from the rotation and enhancement of the magnetic field by eye using WIND plasma and field data and then verified by the geometric parameter fit to the cylindrical constant-alpha force-free field [*Feng et al.*, 2008]. Limited by the date range of the lists available, the distribution of Bs events in these groups is examined from 1995 to 2004.

In order to understand if there is any relationship between Bs events not overlapping with well-defined solar wind structures and well-defined solar wind structures, we examined the temporal separation of Bs events (longer than 1 h and stronger than −5 nT) to solar wind structures. We found that the shortest separation of a Bs event unrelated with well-defined solar wind structure is 20 min from a flux-rope-type Bs event, 15 min from an ejecta Bs event, 10 min from a Shock-type Bs event, and 1 h from a SIR-type Bs event. There are 36 out of 89 MC-type Bs events, seven out of 11 ISMFR-type Bs events, 46 out of 241 ejecta-type Bs events, 48 out of 206 SIR-type Bs events, and eight out of 12 Shock-type Bs events that occur within 3 days of a structure. For the Bs events with separation less than 3 days, the average of the time separation is about 14 h for MC-type Bs events, 27.5 h for ejecta type, and about 36 h for SIR type. We investigated the Bs events that occurred within an hour of a solar wind structures and found that they are distinct intervals rather than part of a complex structure.

The correlation between upstream Bs and geomagnetic activity due to distinct solar wind structures are analyzed using the magnetic field data at 1 AU and geomagnetic indices from CDAWeb. The time shift between WIND and OMNI data is calculated according to *Weimer et al.* [2002]. We define the Bs event

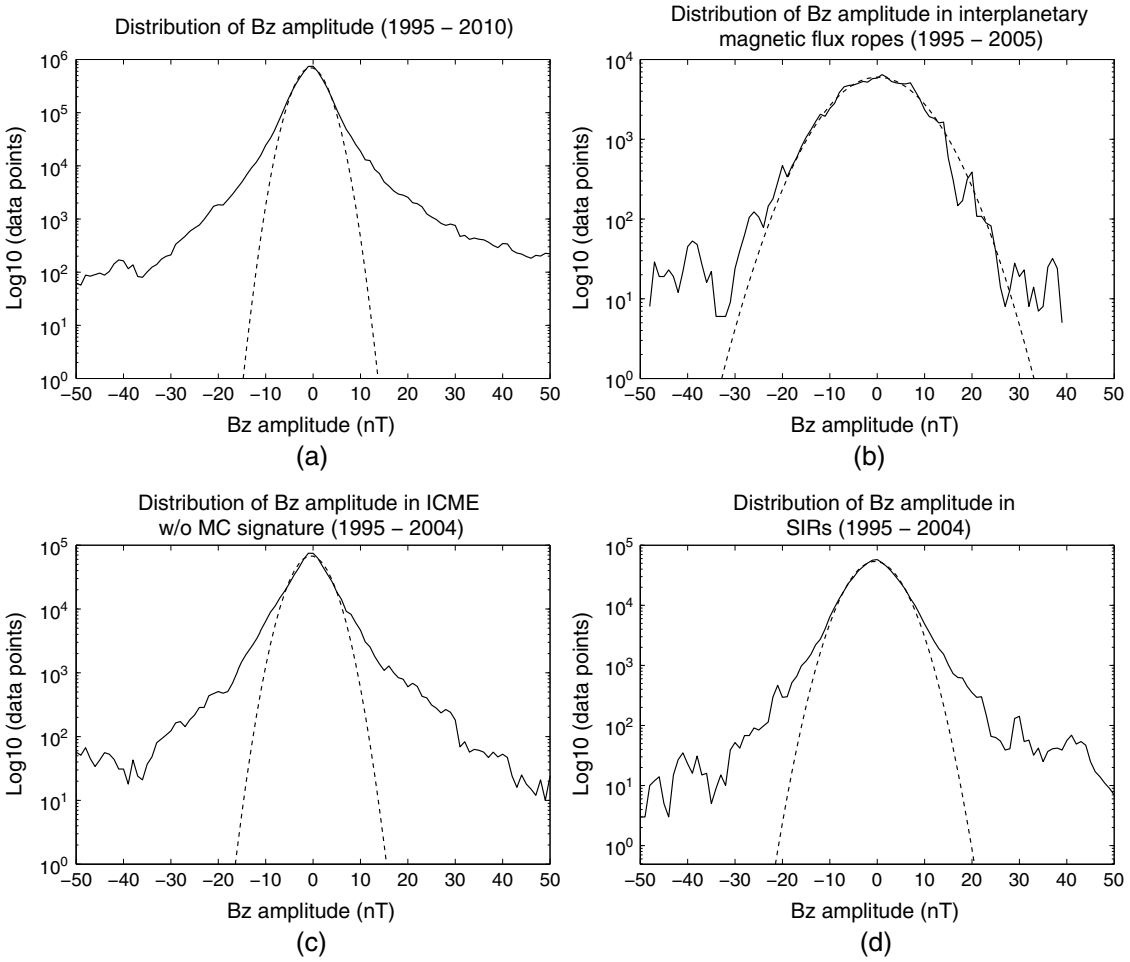

Figure 2. (a) All the data points from 1995 to 2010 (OMNI magnetic field data), (b) interplanetary magnetic flux rope (IMFR, including MC and ISMFR) intervals from 1995 to 2005, (c) ejecta intervals from 1995 to 2004, (d) SIR intervals from 1995 to 2004. The distribution of IMF *Bz* amplitude in GSE coordinates from 1 min WIND magnetometer data (except Figure 2a) is shown as the solid line in each panel, and the dashed lines are the one-peak Gaussian fit.

geoeffective if the SYM-H/AL index decreases below −50/−1000 nT during 1 h following the end of the time-shifted IMF Bs intervals.

For intervals not associated with distinct solar wind structures lasting longer than 6 h, we investigate in detail the plasma and magnetic field properties. We then compare these intervals with the conditions of MHD discontinuities and jump conditions for shocks to preliminarily identify them as slow shock, tangential discontinuity, rotational discontinuity, or unperturbed solar wind.

3. Results

3.1. Statistical Distribution of IMF *Bz*

3.1.1. Distribution of Duration and Amplitude of IMF *Bz*

Figure 2 illustrates the distribution of IMF *Bz* amplitude in GSE coordinates from 1 min WIND magnetometer data (except (a) using OMNI 1 min magnetic field data) (solid line in each panel) and the Gaussian fit (dashed line). Figures 2a includes all the data points from 1995 to 2010, 2b interplanetary magnetic flux rope (IMFR, including MC and ISMFR) intervals from 1995 to 2005, 2c ejecta intervals from 1995 to 2004, and 2d SIR intervals from 1995 to 2004. The results for years in Figures 2a, 2c, and 2d all show one peak at 0 nT with a symmetric distribution of positive and negative values, which fit the Gaussian function well within about ± 10 nT. We examined the data points that have IMF *Bz* less than −10 nT and found that nearly 90% of them occurred in continuous southward IMF intervals with durations longer than 1 h. The distribution of IMFRs in Figure 2(b) has other significant peaks besides 1 nT at more positive and negative *Bz* values than the other categories. The half width of the Gaussian fit function is 20 nT for IMFR, 8 nT for ejecta, 10 nT for SIR, and

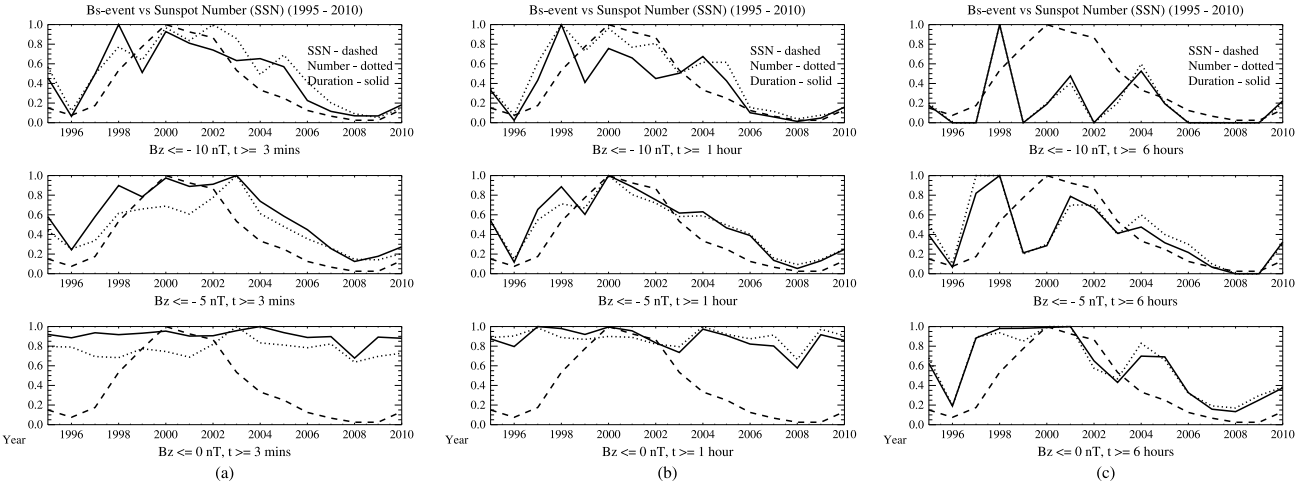

Figure 3. The yearly distribution (divided by the maximum of each parameter) of the number and total duration of Bs events from 1995 to 2010, compared with the sunspot number. The period of the events lasts at least (a) 3 min, (b) 1 h, and (c) 6 h. The upper threshold of the *Bz* value is −10 nT, −54 nT, and 0 nT from the top to the bottom panels in each plot.

6 nT for the whole duration 1995–2010. This indicates that MCs are the dominant source of extreme IMF *Bz* values.

3.1.2. Statistical Properties of IMF Bs Compared to Sunspot Number

Figure 3 presents the normalized yearly distribution (divided by the maximum of each parameter) of the number and total duration of Bs events from 1995 to 2010 (1 min averaged definitive multispacecraft interplanetary magnetic field data from OMNI), compared with the sunspot number. Table 1 shows the minimum and maximum values for variables illustrated in Figure 3. The period of the events lasts at least 3 mins, 1 h, and 6 h in Figures 3a, 3b, and 3c, respectively. The upper threshold of the *Bz* value is −10 nT, −5 nT, and 0 from the top to the bottom panels in each plot. There is a positive correlation shown between the variation of sunspot number and the distribution of IMF Bs properties for the −5 nT and −10 nT cases but no clear correlation for 0 nT. However, the correlation is good for all the events longer than 6 h regardless of the magnitude (shown in Figure 3c). It is also interesting that the maximum of sunspot number does not always match the Bs event maximum from Figure 3. For the Bs events with Bs thresholds less than −10 nT, shown in the first column in Figure 3, the peak of total duration is 1 year ahead of the sunspot number peak. There is a dual-/triple-peak signature in the yearly variation of IMF Bs event number and duration of Bs events. The low occurrence of IMF Bs events from 2007 to 2009 indicates that the most recent solar minimum was prolonged, consistent with sunspot number, which has been shown in previous work [*Russell et al.*, 2010].

Table 1. Minimum and Maximum Values of Variables Illustrated in Figure 3[a]

Variables	Min Count	Max Count	Min Duration (hour)	Max Duration (hour)
Sunspot number	3	120		
(−10 nT, 3 min)	16	307	9	132
(−5 nT, 3 min)	409	2893	87	698
(0 nT, 3 min)	7401	10839	2919	4304
(−10 nT, 1 h)	2	36	1	87
(−5 nT, 1 h)	12	147	17	327
(0 nT, 1 h)	859	1160	1362	2359
(−10 nT, 6 h)	0	5	0	47
(−5 nT, 6 h)	0	10	0	101
(0 nT, 6 h)	8	47	59	441

[a]The numbers in bracket in the first column are the thresholds for intensity and total duration (hours) of Bs events.

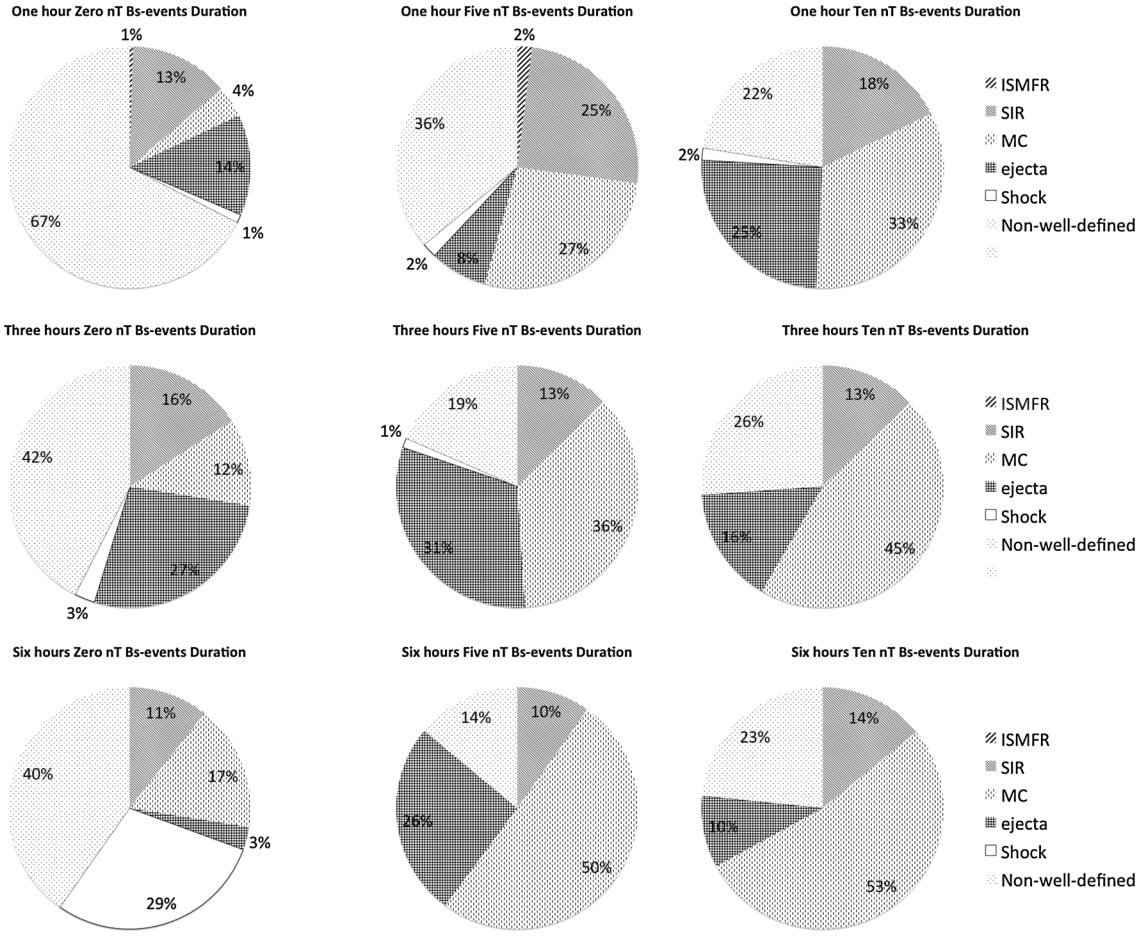

Figure 4. The distribution of total duration of Bs events in MC, ISMFR, ejecta, SIR, Shock, and other cases.The minimum value of IMF Bs magnitude and the event duration is shown at the top of each subfigure. The marker type is shown at the right side of each plot.

3.2. Association of Bs Events With Well-Defined Solar Wind Structures

Figure 4 illustrates the distribution of total duration of Bs events in MC, ISMFR, ejecta, SIR, Shock, and those unrelated with well-defined solar wind structure. The minimum value of IMF Bs magnitude and the event duration are shown at the top of each subfigure. The structure type is shown at the right side in each plot. We find that for the Bs events that last more than 1 h with maximum *Bz* value as zero, the cases unrelated with well-defined solar wind structure are dominant (nearly 70%). As the threshold of the duration and magnitude of Bs increase, the proportion of MC-type Bs events increases. The contribution of ejecta-type Bs events is also smaller as the duration is longer when the maximum *Bz* is −10 nT. The Bs events in the ISMFR group only occur in the category of events with duration less than 1 h and Bs intensity less than 5 nT. The Shock-type Bs events also never exceed 3% of any of the distributions. It is noteworthy that for the Bs events that are longer than 6 h and have minimum Bs value of −10 nT, the MC-type Bs events become the majority (53%); however, nearly one quarter of the intervals are not associated with well-defined structures such as flux ropes, ejecta, SIR, or Shock, and 10% are related to ejecta.

Figure 5 shows scatterplots of minimum SYM-H (nT) in terms of minimum *Bz* and duration for Bs events in different categories: (a) MC, (b) ejecta, (c) SIR, and (d) unrelated with well-defined solar wind structures. The threshold of the duration and Bs magnitude are 1 h and −10 nT. Since there are only five Shock-related events, we do not show it for statistical characteristics. The color bar represent the minimum SYM-H values in the corresponding intervals (with the solar wind time shifted). The duration of MC-type Bs events (shown in Figure 5a) has the largest range from 1 h up to about 13 h, but the minimum *Bz* values are mostly distributed between −10 nT and −30 nT. The minimum SYM-H during the strongest magnetic storm is less than −450 nT while the duration and maximum magnitude of Bs is around 8.5 h and 50 nT, respectively. Over 70%/50% of the MC Bs events triggered a moderate/strong storm (SYM-H < −50/−100 nT). From Figure 5b,

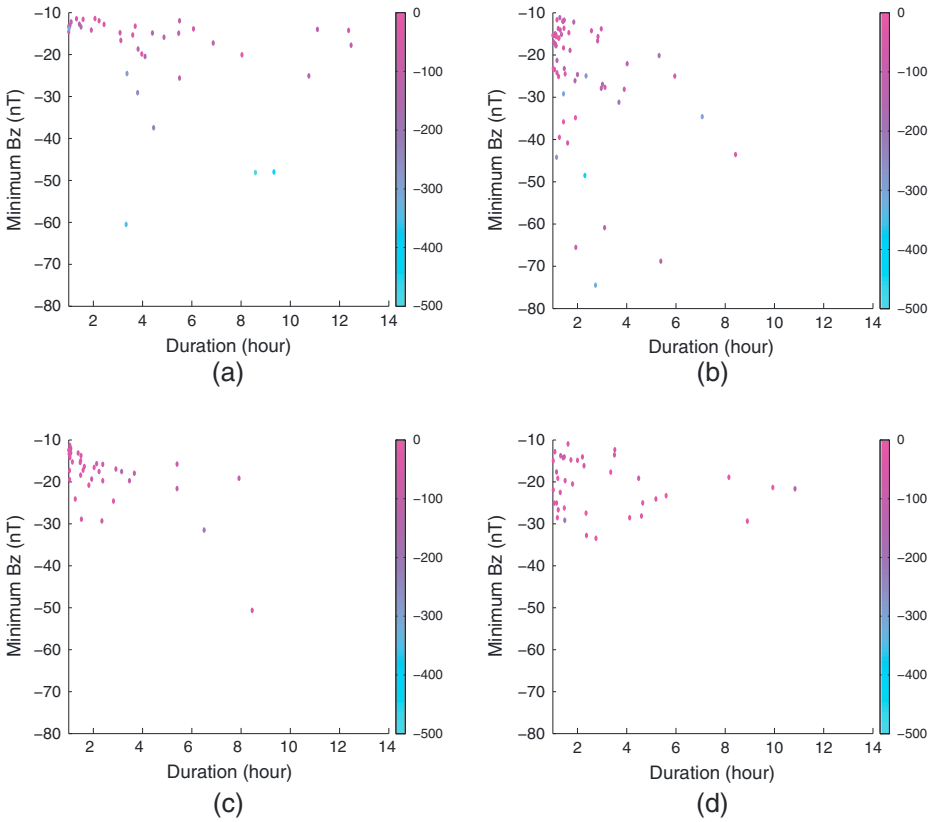

Figure 5. Scatterplots of minimum SYM-H (nT) in terms of minimum *Bz* and duration for Bs events in different categories: (a) MC, (b) ejecta, (c) SIR, and (d) unrelated with well-defined solar wind structures. The threshold of the duration and Bs magnitude are 1 h and 10 nT (There is no ISMFR Bs event for the threshold). The color codes show the minimum SYM-H values in the corresponding intervals (the time shift method is mentioned in section 2.

the minimum *Bz* of ejecta-type Bs events extends to −76 nT, and the duration ranges up to 7 h. The greatest storm identified by the minimum SYM-H (−435 nT) is triggered by an ejecta with duration of 2.3 h and minimum *Bz* of −48.5 nT. Figure 5c shows that 86% of the SIR-type Bs events are distributed in the region $-30\ \text{nT} < \min(Bz) < -10\ \text{nT}$, $1\ \text{h} < \text{duration} < 4\ \text{h}$, while the most intense storm (SYM-H < −200 nT) was related to a Bs event with maximum Bs intensity as −32 nT for about 6.5 h. For the Bs events that are not related with well-defined solar wind structures shown in Figure 5d, the most intense storm with a minimum SYM-H less than −200 nT was triggered by an event with minimum *Bz* around −30 nT and duration of 6.5 h. In the group unrelated with well-defined solar wind structure, intense magnetic storms occurred if either the duration of the Bs event was prolonged or the minimum *Bz* was more negative.

To check the correlation of duration and magnitude with SYM-H index for these Bs events in detail, Figure 6 shows the distribution of minimum SYM-H versus duration (Figures 6a, 6c, and 6e) and minimum *Bz* (Figures 6b, 6d, and 60f) for the same set of MC/SIR/ejecta Bs events in Figure 5. Comparing Figures 6a and 6b, note that for MC Bs events the increase of the magnitude of Bs is more geoeffective than increasing the duration for triggering an intense storm. It is shown from Figures 6c and 6d that for ejecta-type Bs events, there is no significant linear correlation either between minimum *Bz* and minimum SYM-H or between duration and minimum SYM-H. Furthermore, from Figures 6e and 6f, we find that the SIR Bs events are different from the MC-type Bs events: if the duration is longer, even if the minimum *Bz* does not change much, stronger storms can be driven.

3.3. IMF Bs Events Unrelated With Well-Defined Solar Wind Structure

Figure 7 presents the plasma and magnetic field observations at L1 time shifted to the bow shock for Bs events unrelated with well-defined solar wind structures. There is a discontinuity identified at one end of them, marked by the dashed vertical lines and named in the title of each plot. The change of magnitude and direction of magnetic field and velocity, solar wind pressure, and proton number density, as well as the

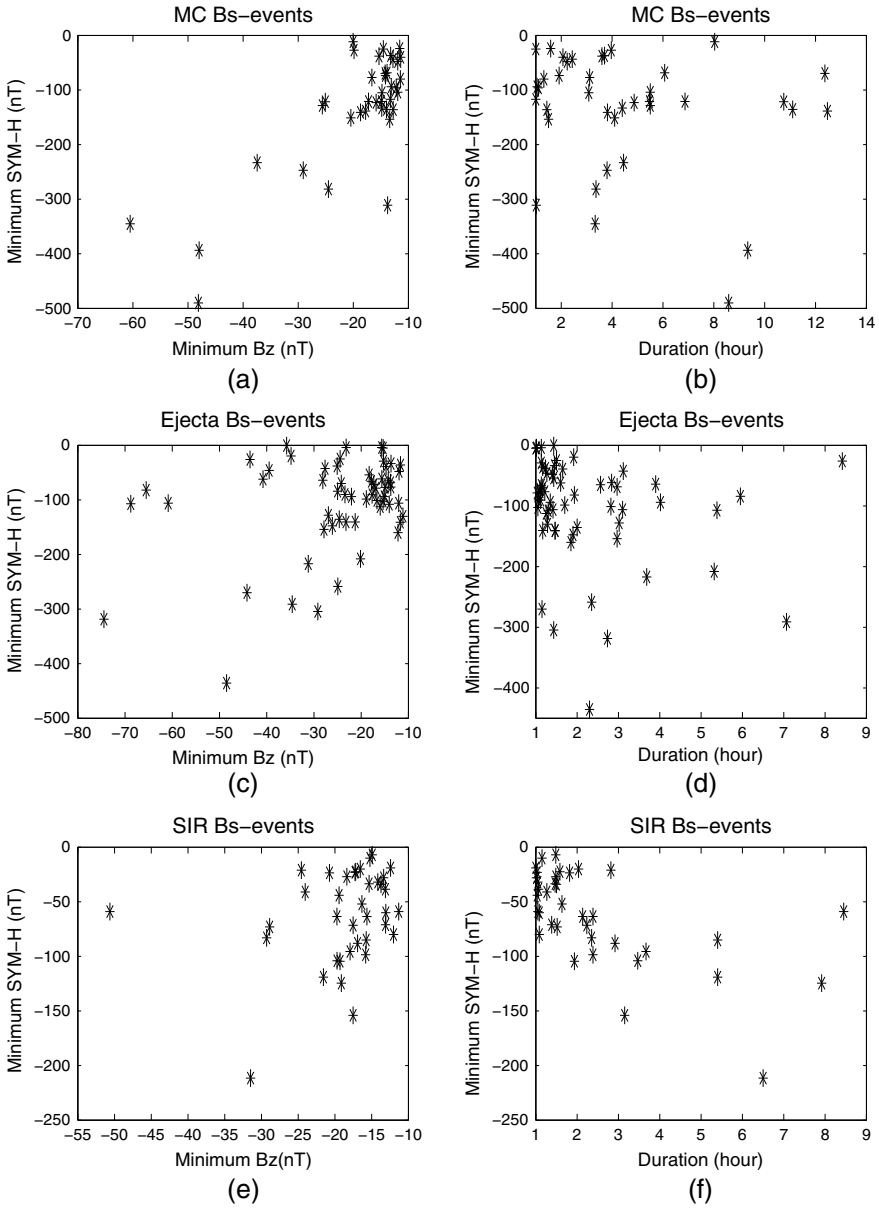

Figure 6. The distribution of (a, c, and e) minimum SYM-H versus minimum *Bz* and (b, d, and f) duration for the same set of MC/SIR/ejecta Bs events in Figure 5.

plasma beta, are the main parameters for identifying the discontinuity types. The first row shows that at about 19:50 UT on 10 November 2001, there was a discontinuity characterized by a slow shock occurring at the beginning of a Bs event not related with a well-defined solar wind structure. The increase of proton number density, dynamic pressure, and plasma beta, combined with the decrease of magnetic field magnitude and solar wind speed, show the features of a slow shock. It is illustrated in the middle plot that on 27 August 1998, a tangential discontinuity occurred at about 05:55 UT, which is indicated by the decrease of proton number density, dynamics pressure, solar wind speed, and plasma beta as well as the increase of the magnetic field intensity. On 6 December 2004, a Bs event is accompanied with a rotational discontinuity at the end (15:20 UT) of the interval that showed no change in magnitude of the magnetic field or velocity, but their direction changed significantly.

In order to study the solar or interplanetary origins of the long-duration, large-amplitude Bs events unrelated with well-defined solar wind structures, we investigated the Bs events that are longer than 6 h case

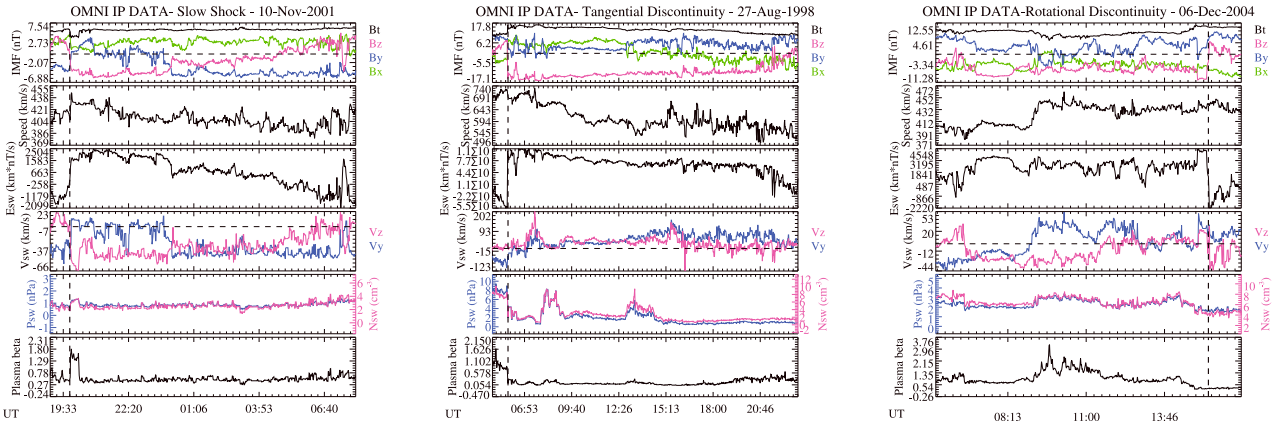

Figure 7. The plasma and magnetic field observations at the bow shock for Bs events with discontinuities identified at one end. The discontinuity is marked by the dashed vertical line and named in the title in each plot.

by case and found that for about 71% (127 out of 179) of these intervals, either or both of the ends are characterized by discontinuity, i.e., tangential discontinuity, rotational discontinuity, or slow shock.

4. Discussion

4.1. Comparison of Yearly Trends of Solar Activity, IMF Bs, and Geomagnetic Activity Indices

Prestes et al. [2006] performed spectral analysis of sunspot number and geomagnetic indices and found that the annual average of antipodal activity (a_a) shows a dual-peak structure, one near sunspot cycle maximum and the other in the descending phase. They proposed that the first peak is caused by CMEs while the second one resulted from coronal hole fast streams. The dual-peak phenomenon is also present in our study for IMF Bs and is more significant if the duration of Bs event is longer. Analyzing the yearly distribution of IMF Bs intervals for different categories, we find that the contribution to the second peak is mainly from the SIR and Bs event unrelated with well-defined solar wind structure. The cross-correlation analysis of sunspot number (Rz) and a_a in *Prestes et al.* [2006] implies that the maximum value of a_a lags that of Rz by a year; however, IMF Bs event occurrence is peaked 1 year ahead of Rz in our results for the main peak. This difference will be investigated in detail in future work.

4.2. Origins of Long-Duration IMF Bs Events Unrelated With Well-Defined Solar Wind Structure

We show that the dominant contribution to the Bs events is not from well-defined solar wind structures (MC, ISMFR, ejecta, SIR, and Shock). We also find that most of the long-duration, large-amplitude intervals unrelated with well-defined solar wind structures began or ended with a discontinuity or slow shock. *Burlaga* [1970] suggested that most discontinuities originate within 0.8 AU and do not evolve appreciably between 0.8 AU and 1.0 AU, other than those generated from the interaction of fast and slow streams near 1 AU. *Whang et al.* [1998] and *Gosling et al.* [2006] also proposed that local, quasi-stationary reconnection occurs relatively frequently in the solar wind and produces Petschck-type exhausts, which could in turn form slow shocks. *Vasquez et al.* [2007] surveyed the small magnetic field discontinuities of Bartels rotation 2286 and found that most discontinuities come from Alfvénic turbulence. If these trends are confirmed, our results show that most long-duration Bs intervals unrelated to ICMEs could be formed in the solar wind or evolved in the interplanetary medium with a solar source for the Alfvénic turbulence. A future study will examine the occurrence frequency of Bs events from satellites inside 1 AU.

4.3. Geoeffectiveness of IMF Bs Events

In order to comprehensively study the geoeffectiveness of the Bs events, we also investigated the maximum *AE* in terms of Bs duration and magnitude (not shown here). The results are that the strongest storm and substorm are not associated with the same event except the ejecta-type Bs events. This may be due to the large expansion of the auroral oval to low latitudes and hence away from the higher-latitude *AE* stations. For large storms, we also note that great Bs events ($t > 3$ h, $Bz < -10$ nT) do not always induce large storms. This might be explained by *Kane* [2010a, 2010b] who showed that the multivariate analysis of *Bz* and *Dst*, with AU, AL, and auroral particle precipitation index POES as additional indices, has higher correlation than *Bz* and only *Dst*, suggesting that the solar wind input energy is distributed to various channels of the Earth's

magnetosphere in addition to the ring current. Another possible mechanism to support the observational result is that the preconditioning of the plasma sheet plays an important role in the response of the inner magnetosphere to solar wind forcing [*Kozyra et al.*, 2002] and also that the frequency of the polarity change of IMF *Bz* significantly alters the state of the inner magnetosphere via buildup of different time scales of the process [*Liemohn et al.*, 2001]. The distribution of solar wind energy into the Earth's magnetosphere will be examined by data-model comparison for the unusual Bs events in future work.

The result showing that MC, ejecta, and SIR drive storms in different ways is consistent with *Borovsky and Denton* [2006] who showed that CME-driven storms are brief with strong *Dst* while SIR-driven storms are of longer duration. In order to examine the other potential parameters in the solar wind that differentiate the geoeffects of MC, ejecta, and SIR, we obtained the average solar wind speed during the Bs events and found that MC Bs events have the largest mean flow speed (512 $\pm$ 195 km/s), ejecta Bs events average 436 $\pm$ 183 km/s, and 379 $\pm$ 89 km/s for SIR. It implies that the co-occurrence of high-speed solar wind in different types of Bs events account for the different behaviors of the Earth's magnetosphere.

5. Summary and Conclusions

We examine the Interplanetary Magnetic Field (IMF) at 1 AU using 1 min magnetic field data from 1995 to 2010. Bs events are defined as continuous periods of southward IMF that satisfy the criteria for magnitude and duration. We also present the statistical properties of IMF Bs events in different groups of solar wind structures and their geoeffectiveness. The results of our study are summarized as follows:

1. The yearly distribution of Bs events shows no correlation with the sunspot number if the threshold magnitude is 0 nT and duration is shorter than 1 h. As the intensity of Bs increases to 5 nT and larger, or the duration is increased to 1 h and longer, the variation of Bs event occurrence is highly correlated with sunspot number.
2. Most Bs events are not associated with well-defined solar wind structures. MC-type Bs events are dominant if the minimum magnitude and duration of Bs is set to be 10 nT and 3 h or 5 nT and 6 h. The Bs events unrelated with well-defined solar wind structure make up a quarter of the long-duration, large-amplitude Bs events ($t > 6$ h, $Bz < -10$ nT), and ejecta-type Bs events constitute 10%.
3. The Bs events with the longest duration and most negative values do not trigger the most intense magnetic storm or substorm, and the strongest storms do not correspond to the strongest substorms except for the MC-type and ejecta-type Bs events. The great Bs events, which are longer than 3 h and greater than -10 nT, are not always related with large storms (minimum SYM-H < -100 nT), indicating that solar wind velocity is also important.

Based on the results and discussion from our study, we conclude that one quarter of extreme IMF Bs events are not related to solar events but related to discontinuities or slow shocks formed in the solar wind by Alfvénic turbulence. Thus, one quarter of geoeffective solar wind conditions currently cannot be predicted from solar observations. Also, MC, ejecta, and SIR can have similar IMF *Bz* properties but due to their solar wind speeds give rise to different geomagnetic responses.

Acknowledgments
This work was supported by NASA grant NNX09A162G. We thank R. Lepping for providing the WIND magnetic field data. We also thank the Harvard-Smithsonian Center for Astrophysics for providing the event list of shocks (http://www.cfa.harvard.edu/shocks/). And we are indebted to NASA Goddard Space Flight Center for providing the Magnetic Cloud event list (http://wind.gsfc.nasa.gov/mfi/mag_cloud_pub1.html).

Philippa Browning thanks the reviewers for their assistance in evaluating this paper.

References

Akasofu, S.-I. (1968), *Polar and Magnetospheric Substorms*, D. Reidel, Norwell, Mass.
Akasofu, S.-I. (1979), A search for the interplanetary quantity controlling the development of geomagnetic storms, *Q. J. R. Astron. Soc.*, *20*, 119–137.
Arnoldy, R. L. (1971), Signature in the interplanetary medium for substorms, *J. Geophys. Res.*, *76*, 5189–5201.
Bobrov, M. S. (1983), Non-recurrent geomagnetic disturbances from high-speed streams, *Planet. Space Sci.*, *31*, 865–870.
Borovsky, J. E., and M. H. Denton (2006), Differences between CME-driven storms and CIR-driven storms, *J. Geophys. Res.*, *111*, A07S08, doi:10.1029/2005JA011447.
Burch, J. L. (1972), Preconditions for the triggering of polar magnetic substorms by storm sudden commencements, *J. Geophys. Res.*, *28*, 5629–5632.
Burlaga, L. F. (1968), Micro-scale structures in the interplanetary medium, *Sol. Phys.*, *4*, 67–92.
Burlaga, L. F. (1970), Discontinuities and shock waves in the interplanetary medium and their interaction with the magnetosphere, in *Solar-Terrestrial Physics/1970, Part II: The Interplanetary Medium*, edited by E. R. Dyer, J. G. Roederer, and A. J. Hundhausen, pp. 135–158, Springer, New York.
Burlaga, L. F., R. M. Skoug, C. W. Smith, D. F. Webb, T. H. Zurbuchen, and A. Reinard (2001), Fast ejecta during the ascending phase of solar cycle 23: ACE observations, 1998–1999, *J. Geophys. Res.*, *106*, 20,957–20,977.
Cane, H. V., and I. G. Richardson (2003), Interplanetary coronal mass ejections in the near-Earth solar wind during 1996–2002, *J. Geophys. Res.*, *108*(A4), 1156, doi:10.1029/2002JA009817.
Dessler, A. J. (1967), Solar wind and interplanetary magnetic field, *Rev. Geophys.*, *5*, 1–41.

Dungey, J. W. (1961), Interplanetary magnetic field and the auroral zones, *Phys. Rev. Lett.*, *6*, 47–48.
Echer, E., W. D. Gonzalez, and B. T. Tsurutani (2008), Interplanetary conditions leading to superintense geomagnetic storms (Dst $\leq$ −250 nT) during solar cycle 23, *Geophys. Res. Lett.*, *35*, L06S03, doi:10.1029/2007GL031755.
Fairfield, D. H., and J. L. J. Cahill (1966), Transition region magnetic field and polar magnetic disturbances, *J. Geophys. Res.*, *71*(1), 155–169.
Feng, H.-Q., D.-J. Wu, C.-C. Lin, J.-K. Chao, L. C. Lee, and L. H. Lyu (2008), Interplanetary small- and intermediate-sized magnetic flux ropes during 1995–2005, *J. Geophys. Res.*, *113*, A12105, doi:10.1029/2008JA013103.
Feng, H.-Q., J.-K. Chao, L. H. Lyu, and L. C. Lee (2010), The relationship between small interplanetary magnetic flux rope and the substorm expansion phase, *J. Geophys. Res.*, *115*, A09108, doi:10.1029/2009JA015191.
Gonzalez, W. D., J. A. Joselyn, Y. Kamide, H. W. Kroehl, G. Rostoker, B. T. Tsurutani, and V. M. Vasyliunas (1994), What is a geomagnetic storm?, *J. Geophys. Res.*, *99*, 5771–5792.
Gosling, J. T. (1993), The solar flare myth, *J. Geophys. Res.*, *98*, 18,937–18,949.
Gosling, J. T., S. Eriksson, and R. Schwenn (2006), Petschek-type magnetic reconnection exhausts in the solar wind well inside 1 AU: Helios, *J. Geophys. Res.*, *111*, A10102, doi:10.1029/2006JA011863.
Henderson, M. G., G. D. Reeves, R. D. Belian, and J. S. Murphree (1996), Observations of magnetospheric substorms occurring with no apparent solar wind/IMF trigger, *J. Geophys. Res.*, *101*, 10,773–10,791.
Heppner, J. P. (1955), Note on the occurrence of world-wide S.S.C.'s during the onset of negative bays at College, Alaska, *J. Geophys. Res.*, *60*, 29–32.
Hirshberg, J., and D. S. Colburn (1969), Interplanetary field and geomagnetic variations—A unified view, *Planet. Space Sci.*, *17*, 1183–1206.
Hochedez, J.-F., A. Zhukov, E. Robbrecht, R. V. der Linden, D. Berghmans, P. Vanlommel, A. Theissen, and F. Clette (2005), Solar weather monitoring, *Ann. Geophys.*, *23*, 3149–3161.
Horwitz, J. L. (1985), The substorm as an internal magnetospheric instability: Substorms and their characteristic time scales during intervals of steady interplanetary magnetic field, *J. Geophys. Res.*, *90*, 4164–4170.
Jian, L. K., C. Russell, J. G. Luhmann, and R. M. Skoug (2006a), Properties of stream interactions at one AU during 1995–2004, *Sol. Phys.*, *239*, 337–392.
Jian, L. K., C. Russell, J. G. Luhmann, and R. M. Skoug (2006b), Properties of interplanetary coronal mass ejections at one AU during 1995–2004, *Sol. Phys.*, *239*, 393–436.
Jian, L. K., C. Russell, J. G. Luhmann, P. J. MacNeice, D. Odstricil, P. Riley, J. A. Linker, R. M. Skoug, and J. T. Steinberg (2011), Comparison of observations at ACE and Ulysses with Enlil model results: Stream interaction regions during Carrington rotations 2016–2018, *Sol. Phys.*, *273*, 179–203.
Jurac, S., J. C. Kasper, J. D. Richardson, and A. J. Lazarus (2002), Geomagnetic disturbances and their relationship to interplanetary shock parameters, *Geophys. Res. Lett.*, *29*(10), 1463, doi:10.1029/2001GL014034.
Kane, R. P. (2010a), Relationship between the geomagnetic Dst(min) and the interplanetary Bz(min) during cycle 23, *Planet. Space Sci.*, *58*, 392–400.
Kane, R. P. (2010b), Scatter in the plots of Dst(min) versus Bz(min), *Planet. Space Sci.*, *58*, 1792–1801.
Klein, L. W., and L. F. Burlaga (1982), Interplanetary magnetic clouds at 1 AU, *J. Geophys. Res.*, *87*, 613–624.
Kozyra, J. U., M. W. Liemohn, C. R. Clauer, A. J. Ridley, M. F. Thomsen, J. E. Borovsky, J. L. Roeder, V. K. Jordanova, and W. D. Gonzalez (2002), Multistep *Dst* development and ring current composition changes during the 4–6 June 1991 magnetic storm, *J. Geophys. Res.*, *107*(A8), 1224, doi:10.1029/2001JA000023.
Lepping, R. P., L. F. Burlaga, and J. A. Jones (1990), Magnetic field structure of interplanetary magnetic clouds at 1 AU, *J. Geophys. Res.*, *95*, 11,957–11,965.
Liemohn, M. W., J. U. Kozyra, M. F. Thomsen, J. L. Roeder, G. Lu, J. E. Borovsky, and T. E. Cayton (2001), The dominant role of the asymmetric ring current in producing the stormtime *Dst**, *J. Geophys. Res.*, *106*, 10,883–10,904.
Lindsay, G. M., C. T. Russell, and J. G. Luhmann (1995), Coronal mass ejection and stream interaction region characteristic and their potential geomagnetic effectiveness, *J. Geophys. Res.*, *10*, 16,999–17,013.
Lindsay, G. M., J. G. Luhmann, C. T. Russell, and J. T. Gosling (1999), Relationships between coronal mass ejection speeds from coronagraph images and interplanetary characteristics of associated interplanetary coronal mass ejections, *J. Geophys. Res.*, *104*, 12,515–12,523.
Lyons, L. R. (1995), A new theory for magnetospheric substorms, *J. Geophys. Res.*, *100*, 19,069–19,081.
Lyons, L. R. (1996), Substorms: Fundamental observational features, distinction from other disturbances, and external triggering, *J. Geophys. Res.*, *101*, 13,011–13,026.
Moldwin, M. B., S. Ford, R. Lepping, J. Slavin, and A. Szabo (2000), Small-scale magnetic flux ropes in the solar wind, *Geophys. Res. Lett.*, *27*, 57–60.
Mursula, K., and B. Zieger (1996), The 13.5-day periodicity in the Sun, solar wind, and geomagnetic activity: The last three solar cycles, *J. Geophys. Res.*, *101*, 27,077–27,090.
Prestes, A., N. R. Rigozo, E. Echer, and L. E. A. Vieira (2006), Spectral analysis of sunspot number and geomagnetic indices (1868–2001), *J. Atmos. Sol. Terr. Phys.*, *68*, 182–190.
Richardson, I. G., and H. V. Cane (2012), Near-Earth interplanetary coronal mass ejections during solar cycle 23 (1996–2009): Catalog and summary of properties, *Sol. Phys.*, *264*, 189–237.
Rosenberg, R. L., and J. P. J. Coleman (1980), Solar cycle-dependent north-south field configurations observed in solar wind interaction regions, *J. Geophys. Res.*, *85*, 3021–3032.
Russell, C. T., J. G. Luhmann, and L. K. Jian (2010), How unprecedented a solar minimum?, *Rev. Geophys.*, *48*, RG2004, doi:10.1029/2009RG000316.
Samson, J. C., and K. L. Yeung (1986), Some generalizations on the method of superposed epoch analysis, *Planet. Space Sci.*, *34*, 1133–1142.
Schwadron, N. A., and D. J. McComas (2004), The sheared sub-Parker spiral, Abstract SH34A-04 presented at 2004 Fall Meeting, AGU, San Francisco, Calif.
Sheeley, J. N. R., J. W. Harvey, and W. C. Feldman (1976), Coronal holes, solar wind streams, and recurrent geomagnetic disturbances: 1973–1976, *Sol. Phys.*, *49*, 271–278.
Tsurutani, B. T., and W. D. Gonzalez (1987), The cause of high intensity long-duration continuous AE activity (HILDCAAs): Interplanetary Alfvén wave trains, *Planet. Space Sci.*, *35*, 405–412.
Vasquez, B. J., V. I. Abramenko, D. K. Haggerty, and C. W. Smith (2007), Numerous small magnetic field discontinuities of Bartels rotation 2286 and the potential role of Alfvénic turbulence, *J. Geophys. Res.*, *112*, A11102, doi:10.1029/2007JA012504.
Webb, D. F. (1991), The solar cycle variation of the rates of CMEs and related activity, *Adv. Space Res.*, *11*, 37–40.

Weimer, D. R., D. M. Ober, N. C. Maynard, W. J. Burke, M. R. Collier, D. J. McComas, N. F. Ness, and C. W. Smith (2002), Variable time delays in the propagation of the interplanetary magnetic field, *J. Geophys. Res.*, *107*(A8), 1210, doi:10.1029/2001JA009102.

Whang, Y. C., D. Larson, R. P. Lin, R. P. Lepping, and A. Szabo (1998), Plasma and magnetic field structure of a slow shock: Wind observations in interplanetary space, *Geophys. Res. Lett.*, *25*, 2625–2628.

Xu, D., T. Chen, X.-X. Zhang, and Z. Liu (2009), Statistical relationship between solar wind conditions and geomagnetic storms in 1998–2008, *Planet. Space Sci.*, *57*, 1500–1513.

Yashiro, S., N. Gopalswamy, G. Michalek, O. C. St. Cyr, S. P. Plunkett, N. B. Rich, and R. A. Howard (2004), A catalog of white light coronal mass ejections observed by the SOHO spacecraft, *J. Geophys. Res.*, *109*, A07105, doi:10.1029/2003JA010282.

Zhang, X.-Y., M. B. Moldwin, and M. Cartwright (2012), The geo-effectiveness of interplanetary small-scale magnetic flux ropes, *J. Atmos. Sol. Terr. Phys.*, *95-96*, 1–14.

Zhou, X., and B. T. Tsurutani (2001), Interplanetary shock triggering of nightside geomagnetic activity: Substorms, pseudobreakups, and quiescent events, *J. Geophys. Res.*, *106*, 18,957–18,967.